How to cite: *Angew. Chem. Int. Ed.* **2024**, *63*, e202318849
doi.org/10.1002/anie.202318849

VIP Enzymes Very Important Paper

N-Cyanopiperazines as Specific Covalent Inhibitors of the Deubiquitinating Enzyme UCHL1

Mirko Schmidt[+], *Christian Grethe*[+], *Sarah Recknagel, Gian-Marvin Kipka, Nikolas Klink, and Malte Gersch**

Abstract: Cyanamides have emerged as privileged scaffolds in covalent inhibitors of deubiquitinating enzymes (DUBs). However, many compounds with a cyanopyrrolidine warhead show cross-reactivity toward small subsets of DUBs or toward the protein deglycase PARK7/DJ-1, hampering their use for the selective perturbation of a single DUB in living cells. Here, we disclose *N*'-alkyl,*N*-cyanopiperazines as structures for covalent enzyme inhibition with exceptional specificity for the DUB UCHL1 among 55 human deubiquitinases and with effective target engagement in cells. Notably, transitioning from 5-membered pyrrolidines to 6-membered heterocycles eliminated PARK7 binding and introduced context-dependent reversibility of the isothiourea linkage to the catalytic cysteine of UCHL1. Compound potency and specificity were analysed by a range of biochemical assays and with a crystal structure of a cyanopiperazine in covalent complex with UCHL1. The structure revealed a compound-induced conformational restriction of the cross-over loop, which underlies the observed inhibitory potencies. Through the rationalization of specificities of different cyanamides, we introduce a framework for the investigation of protein reactivity of bioactive nitriles of this compound class. Our results represent an encouraging case study for the refining of electrophilic compounds into chemical probes, emphasizing the potential to engineer specificity through subtle chemical modifications around the warhead.

[*] Dr. M. Schmidt,[+] Dr. C. Grethe,[+] S. Recknagel, G.-M. Kipka, N. Klink, Dr. M. Gersch
Chemical Genomics Centre
Max-Planck-Institute of Molecular Physiology
Otto-Hahn-Str. 15, D-44227 Dortmund, Germany
E-mail: malte.gersch@mpi-dortmund.mpg.de

Dr. M. Schmidt,[+] Dr. C. Grethe,[+] S. Recknagel, G.-M. Kipka, N. Klink, Dr. M. Gersch
Department of Chemistry and Chemical Biology
TU Dortmund University
Otto-Hahn-Str. 15, D-44227 Dortmund, Germany
E-mail: malte.gersch@tu-dortmund.de

[+] These authors contributed equally to this work.

Introduction

Covalently acting small molecules equipped with electrophilic moieties are invaluable tools in chemical biology to explore the modulation of a wide variety of enzymes.[1–5] However, their intrinsic chemical reactivity can lead to promiscuous targeting of diverse sets of proteins in cells, requiring thorough characterisation.[1,6] Mild electrophiles as warheads such as nitriles (in the form of alkyl or aryl nitriles and cyanamides) offer an attractive avenue for achieving greater selectivity within a range of potential binding sites. Among those, cyanamides have recently garnered attention as privileged scaffolds for the selective targeting of active site cysteines of different classes of deubiquitinases (DUBs).[7–14] These enzymes can remove ubiquitin molecules from target proteins and thereby act as counterplayers of E3 ligases, critically influencing signalling within the ubiquitin-proteasome system.[15–18] The relevance of nitrile-based DUB inhibitors is illustrated by the successful completion of the first clinical trial of a cyanopyrrolidine on USP30 in 2023, demonstrating the translational potential of both this substance class and of deubiquitinating enzymes as therapeutic targets.[12,16] Moreover, bicyclic cyanamides[19,20] with nanomolar potencies on USP30 were reported, of which compound MTX115325 protected dopaminergic neurons in a Parkinson's disease mouse model.[19] In addition, nitriles have been reported as covalent inhibitors of Cathepsins,[21] of dipeptidyl peptidase 4 in anti-diabetic drugs,[22] and of the main protease of SARS-CoV-2 in the drug paxlovid.[23]

Individual cyanopyrrolidine-based DUB probes[7–14] as well as larger cyanamide collections[24–26] have been reported (Figure S1A). These have been employed for highly potent target engagement in cells and in vivo, activity-based profiling of many DUBs in parallel in a cellular environment, and the selective targeting of subsets of DUBs and of non-DUB enzymes. Collectively, these molecules serve as potent tools to shed light on the biological functions of DUBs and their potential roles as therapeutic targets. However, their use is often hampered through unclear specificity, cross-reactivity with other DUBs and non-DUB proteins as well as off-target toxicity. We recently reported on a chemogenomic pair[11,27] of cyanopyrrolidine-based probes to specifically investigate UCHL1-mediated effects (Figure 1A–B), however, the main compound still showed cross-reactivity with the protein deglycase PARK7 (also known as DJ-1) which is typically observed in unbiased, covalent target deconvolution for cyanamides of the 3-carboxypyrrolidine scaffold.[9–11]

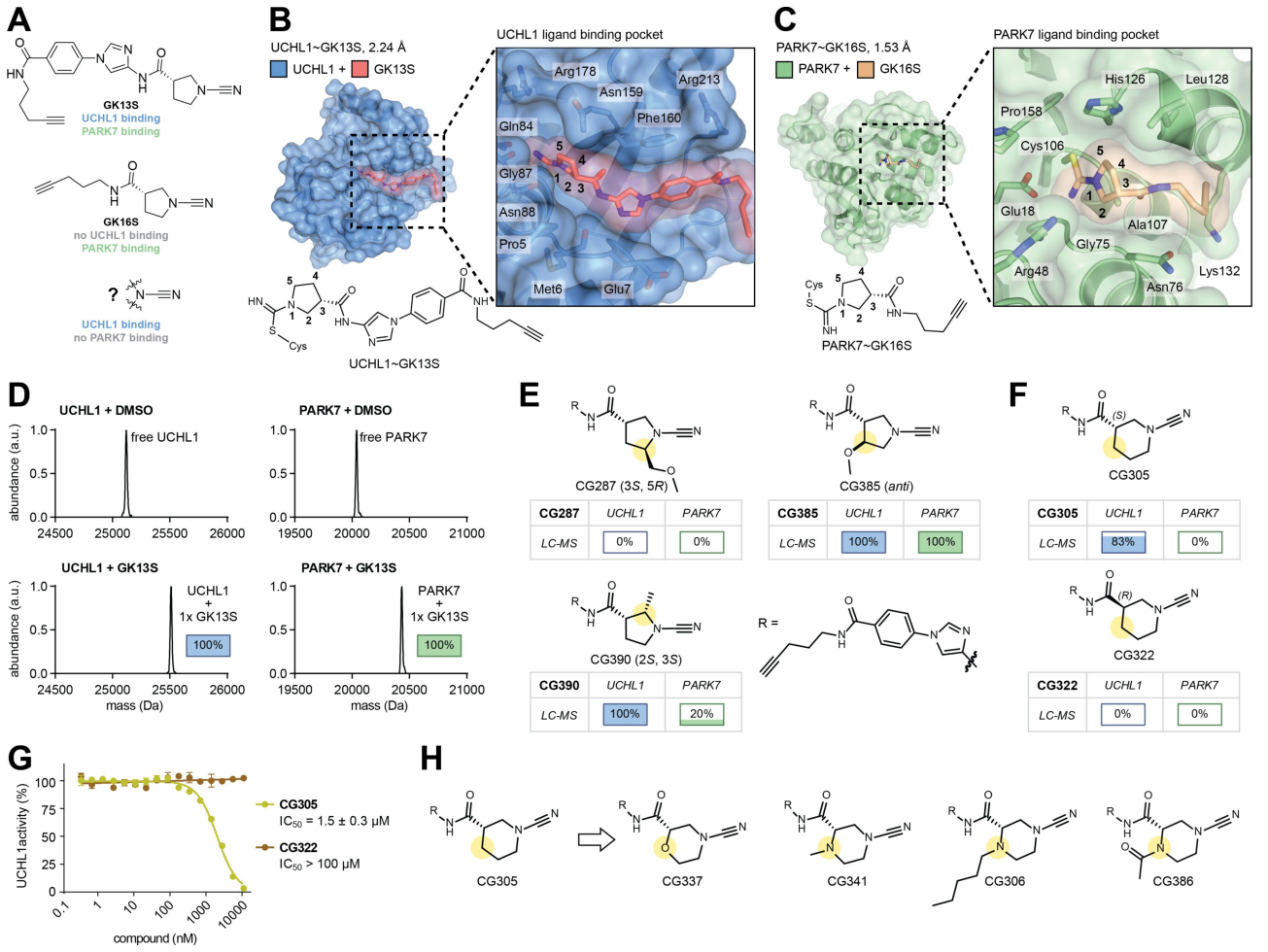

Figure 1. Optimising UCHL1 over PARK7 selectivity in covalent cyanamide inhibitors. A.) Previously reported chemogenomic pair of probes for UCHL1 comprising GK13S and its minimal probe GK16S. B.) Crystal structure of UCHL1 in complex with GK13S and zoom into the binding site with important residues indicated. Atoms of the pyrrolidine ring are numbered. C.) Crystal structure of PARK7~GK16S shown as in B. D.) Intact protein mass spectrometry assay to assess covalent binding of GK13S to recombinant UCHL1 or PARK7. Proteins (3 µM) were treated with compound (10 µM) or DMSO for 1 h prior to analysis. Differences in area-under-the-curve values between samples were calculated and illustrated in blue (for UCHL1) or green (for PARK7) boxes, where 100% relates to full protein labelling. E.) Structures of GK13S derivatives (structural changes highlighted in yellow) and quantification of UCHL1 and PARK7 binding as shown in D. Respective LC–MS data are shown in Figure S3. F.) Equivalent analysis of *N*-cyanopiperidines CG305 and CG322. G.) Assessment of UCHL1 inhibitory potency of *N*-cyanopiperidines in a Ubiquitin-RhoG cleavage assay. Data points are shown as mean ± standard deviation (N = 3). IC_{50} values were determined from 5 (CG305) or 3 (CG322) independent experiments. H.) Chosen optimization strategy based on CG305 with 6-membered ring warheads.

While the precise molecular roles of UCHL1[28–32] and PARK7[33] are still poorly understood, various catalytic mechanisms have been proposed and linked to disease-associated phenotypes.[31,34] In addition, mutations in either enzyme in humans are causative for different forms of neurodegeneration,[29,35] and both enzymes are considered drivers of oncogenic transformation in different contexts.[28,34,36] As such, access to nontoxic, UCHL1-specific small molecule probes is of paramount importance to the field to interrogate its biological roles separately from PARK7 and without cross-reactivity with other DUBs even upon prolonged treatment of cells. In addition, a better molecular understanding of the protein selectivity mechanism of cyanamides is urgently needed to guide the rational improvement of compound properties. Here, we describe *N*-cyanopiperazines as covalent protein inhibitors and introduce CG341 and CG306 for the selective perturbation of UCHL1 in live cells. Extensive biochemical characterisation is complemented with a structural investigation of the protein reactivity of cyanamides, bringing closer the rational engineering of specificity in covalently acting small molecule probes.

Results and Discussion

Suppressing PARK7 reactivity of N-cyanopyrrolidines

Specificity of covalent inhibitors is typically altered either by chemical tuning of the warhead or by changing the specificity element adjacent to the reactive group. Since both minimal *N*-cyanopyrrolidines GK16S and its enantiom-

er GK16R showed pronounced reactivity towards PARK7 both in vitro and in cells,[11] we envisioned that alterations at the *N*-cyanopyrrolidine core may suppress recognition by PARK7. To identify such modifications in a structure-guided approach, we sought to characterise the recognition of both compounds by PARK7. We obtained crystal structures of GK16S (Figure 1C) and of its enantiomer GK16R (Figure S1B) in covalent complex with PARK7 to 1.53 Å and 1.48 Å resolution (Table S1). The pyrrolidine rings were well resolved in both structures (Figure S1C–D) and largely buried in a narrow, hydrophobic cleft formed by Ala107, Gly75, His126, and Leu128, which together spatially restrict access to the nucleophilic Cys106 (Figure S1E). In both structures, carbon atoms 2 and 5 of the pyrrolidine ring are surrounded by protein residues, while atom 4 is solvent accessible. Apart from a rotation of the Asn76 side chain, no structural changes were observed compared to PARK7 in its apo form (Figure S1F). This narrow binding sites appears rather rigid as also no changes were observed in comparison to larger[36] (Figure S1G) or structurally more diverse[37] (Figure S1H) covalent PARK7 inhibitors.

To quantitatively assess compound specificity, we optimized an intact protein mass spectrometry assay reporting on the proportions of covalently modified proteins. In this assay, recombinant UCHL1 and PARK7 were separately incubated with 10 μM of compound for 1 h prior to analysis. Under those conditions, GK13S led to complete modification of both proteins (Figure 1D). In a search for compounds which retain reactivity with UCHL1 but do not react with PARK7, we analysed the binding interfaces of GK13S with UCHL1 (Figure 1B) and of GK16S with PARK7 (Figure 1C). We next synthesized GK13S derivatives with additional steric bulk at carbon atoms 2 (CG390), 4 (CG385) or 5 (CG287) (Figure 1E, Schemes S1,S2,S3). We retained the *S*-configuration of the stereocenter at atom 3 in line with the previous observation that this is required for potent UCHL1 inhibition.[11,36] The covalent protein target spectrum of these compounds was then investigated with activity-based protein profiling (ABPP) in live HEK293 cells (Figure S2A) and in HEK293 cell lysate (Figure S2B). CG390 stood out as it showed a strong and clean labelling profile consistent with UCHL1 modification, whereas both CG287 and CG385 displayed weaker and less selective protein labelling. To specifically investigate UCHL1 engagement, we utilized a competitive assay in which cells (Figure S2C) or cell lysate (Figure S2D) are treated with compound, followed by incubation with the Ubiquitin vinyl sulfone probe HA-Ub-VS which modifies free UCHL1 and therefore makes it distinguishable from inhibitor-bound forms. Consistent with the labelling profile, CG390 potently inhibited UCHL1 under the conditions tested (Figure S2C–D). Since a similar target engagement assay is not available for PARK7, we reverted to the in vitro mass spectrometry assay. Profiling of the compounds revealed that substitution at atom 5 (compound CG287) directly adjacent to the cyanamide warhead was not tolerated by either enzyme, whereas modification at atom 4 (CG385) did not lead to discrimination (Figure 1E, Figure S3A). A methyl group at carbon atom 2 in *S*-configuration (CG390) in vitro suppressed PARK7 reactivity, consistent with a predicated clash with Gly75 (Figure 1C). Although the analysis through the intact protein mass spectrometry assay was largely in agreement with the cellular assays, we were concerned that CG390 showed reduced, but still robustly detectable modification of PARK7 (Figure 1E, S3A) and that this would preclude clean separation of biological activities.

We therefore introduced steric bulk in a different way by synthesizing the piperidine analogues CG305 and CG322 (Schemes S4,S5). No binding to PARK7 was detectable for either compound, while CG305 lead to substantial covalent modification of UCHL1 (Figure 1F, Figure S3B). Consistent with these results, we found that only *S*-configured CG305 inhibited UCHL1 activity (Figure 1G). While the inhibitory potency (IC_{50} of CG305 after 1 hour of incubation under standardized conditions: 1.5 ± 0.3 μM) was decreased by approx. one order of magnitude through the change from pyrrolidine (GK13S) to piperidine (CG305), these data suggest that this activity is primarily driven by specific recognition of the compound by UCHL1 rather than through the mild electrophilicity of the nitrile, as the presence of a cyanamide in CG322 was not sufficient for any activity.

N-Cyano,N'-alkyl piperazines as enzyme inhibitors

Taking CG305 as a starting point for compound optimization to increase UCHL1 potency (Figure 1H), we designed four structural analogues by replacing the piperidine with morpholine (CG337), *N*-methyl piperazine (CG341), *N*-pentyl piperazine (CG306) and *N*-acetyl piperazine (CG386). The aliphatic heterocycles were fused to the phenyl imidazole specificity elements through two synthetic routes, followed by installation of the electrophilic cyanamide with cyanogen bromide (Figure 2A–B and Schemes S6,S8,S10,S15). In order to assess the reactivity of the cyanamide in isolation, we also prepared the respective minimal probes CG365, CG374 and CG375, which lack the aromatic portion of their respective counterparts (Figure 3A, Schemes S7,S9,S11).

We next comprehensively characterized all compounds in a variety of in vitro assays (Figure 3, Figure S4). Notably, both *N*-alkyl piperazines displayed complete modification of UCHL1, but still did not react with PARK7 (Figure 3A, Figure S4A–C). Excitingly, the introduction of an additional heteroatom into the ring of CG305 increased the UCHL1 inhibitory potency with an IC_{50} value of 494 nM for morpholine-containing CG337 and further down to 191 nM and 254 nM for piperazines CG341 and CG306 (Figure 3A–B). These changes in potency could also be recapitulated in an intact protein mass spectrometry assay conducted at lower compound concentration (Figure S4D) as well as through measurements of catalytic inactivation ($k_{obs}/[I]$ values, Figure S5A–C). Moreover, both piperazines showed protein stabilization of UCHL1 in a thermal shift assay, which exceeded the stabilization mediated by GK13S (Figure 3C). Consistent with the notion of their specific recognition by UCHL1, all minimal probes lacked the ability to increase

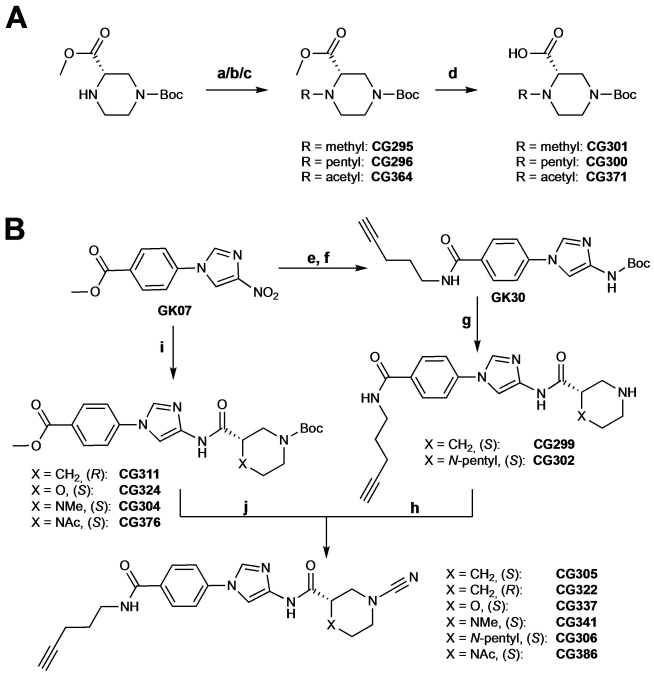

Figure 2. Synthesis of piperidine, morpholine and piperazine analogues of GK13S. A.) Synthesis of piperazine precursors. a.) Formaldehyde, $NaBH(OAc)_3$, AcOH, ACN:MeOH (1:1), rt, on. CG295: 66%. b.) Valeraldehyde, $NaBH(OAc)_3$, AcOH, DCM, rt, on. CG296: 95%. c.) Acetyl chloride, Et_3N, DCM, 0 °C -> rt, on. CG364: 52%. d.) LiOH, 1,4-dioxane, 50 °C, 4 h. B.) Compounds were synthesized using two similar procedures (left and right paths). e.) 1. Pd/C, H_2, EtOH, rt, 5 h. 2. Boc_2O, DIPEA, EtOH, MeOH, rt, 20 h, 20%. f.) 1. LiOH, MeOH, 50 °C, 5 h. 2. Pent-4-yn-1-amine, HATU, DIPEA, DCM, rt, 1 d, 80%. g.) 1. 20% TFA/DCM, rt, 4 h. 2a. for CG299: 1-Boc-L-nipecotic acid, HATU, DIPEA, THF, rt, on. 2b. for CG302: CG300, HATU, DIPEA, THF, rt, on. 3. 20% TFA/DCM, rt, 3 h. CG299: 31%, CG302: 18%. h.) BrCN, K_2CO_3, DMF, rt, 1–2 h. CG305: 77%, CG306: 53%. i.) 1. Pd/C, H_2, EtOH, rt, 5 h. 2a. for CG311: 1-Boc-D-nipecotic acid, HATU, DIPEA, DMF, rt, on, 99%. 2b. for CG324: (*S*)-4-Boc-morpholine-2-carboxylic acid, HATU, DIPEA, DMF, rt, on, 51%. 2c. for CG304: CG301, HATU, DIPEA, DMF, rt, on, 68%. 2d. for CG376: CG371, HATU, DIPEA, DMF, rt, on, 70%. j.) 1. LiOH, 1,4-dioxane, 50 °C, 4–6 h. 2. Pent-4-yn-1-amine, HATU, DIPEA, DMF, rt, on. 3. 20% TFA/DCM, rt, 2–3 h. 4. BrCN, K_2CO_3, DMF, rt, 2–3 h. CG322: 29%, CG337: 17%, CG341: 37%, CG386: 49%.

the protein melting temperature. We previously described that specificity windows of covalent cyanamide probes, as obtained from in vitro assays, may overestimate the specificity observable in complex proteome and with longer incubation times.[11] We were therefore particularly gratified to see that, unlike GK16S, six-membered ring-containing minimal probes lacked any inhibition or covalent modification of UCHL1 (Figure 3). Collectively, these results yielded the *N*-Cyano,*N'*-alkyl piperazines CG341 and CG306 with potent UCHL1 inhibitory activity (approx. 3–4-fold reduced compared to the pyrrolidine equivalent GK13S, yet still at ~200 nM), elevated UCHL1 stabilisation and no PARK7 off-targeting reactivity.

Cellular investigation of N-Cyano,N'-alkyl piperazines

We next set out to test if these in vitro data also reflect compound specificity in cells. We therefore conducted an activity-based protein profiling experiment for which HEK293 cells were treated with compounds for 24 h and covalent protein-compound conjugates were visualized by copper-catalysed click chemistry. While GK13S led to a strong UCHL1 band and the characteristic PARK7-derived band at a slightly lower molecular weight, to our surprise, less intense bands were visible for all probes made of 6-membered rings (Figure S6A). In particular both piperazine-based probes showed barely any protein labelling. This effect was even more pronounced when cell lysates were labelled (Figure S6B). However, when we directly assessed UCHL1 target engagement through the HA-Ub-VS competition assay, we consistently observed near complete inhibition of endogenous UCHL1 by CG341 and CG306 both in cells (Figure 4A) and in cell lysate (Figure S6C). These results demonstrate that the piperazine-based probes are indeed able to efficiently inhibit cellular UCHL1 but are refractory to the activity-based protein profiling workflow. To explore this phenomenon further, we reconstituted the workflow with recombinant protein, and could recapitulate the observation (Figure S6D–E). The experiment revealed an unexpected stability difference of the isothiourea conjugates formed between the catalytic cysteine of UCHL1 and of the cyanamide which critically depends on the ring size. Addition of the click chemistry reagents led to reversal of the covalent bond selectively for cyanamides in 6-membered rings, leading to regenerated free UCHL1 and precluding the visualization of covalently bound protein species (Figure S6E).

To characterise covalent protein targets of the cyanopiperazines in cells in an orthogonal manner, we synthesized non-alkyne-containing analogues of the cyanopiperazines (CG383 for CG341; CG382 for CG306) and utilized those in parallel to alkyne-free versions of the cyanopyrrolidines (CG370S for GK16S; CG118 for GK13S) in a compound-based competition assay (Figure 4B, Schemes S12,S13,S14). Cells were first treated with alkyne-free compounds for 24 h, followed by the addition of alkyne-tagged GK13S for 24 h and activity-based protein profiling (Figure 4C). This experiment demonstrated that, in line with the UCHL1 target engagement assay, cyanopiperazines CG383 and in particular CG382 were able to inhibit UCHL1 to a similar extend as the cyanopyrrolidine CG118, while all other bands were unaffected. Importantly, while CG370S led to a decrease of the PARK7 band intensity, suggesting substantial PARK7 inhibition, both cyanopiperazines did not. However, we noted that several bands in the CG118-pretreated sample remained unaffected, which could be due to short protein half-lives or due to sub-stoichiometric labelling during the first treatment. Therefore, while the experiment did not suggest piperazines to bind GK13S targets including PARK7, it also did not firmly disprove it.

To directly test whether cyanopiperazines engage PARK7 in cells, we optimized a pull-down assay. To this end, we scouted a variety of click chemistry conditions to

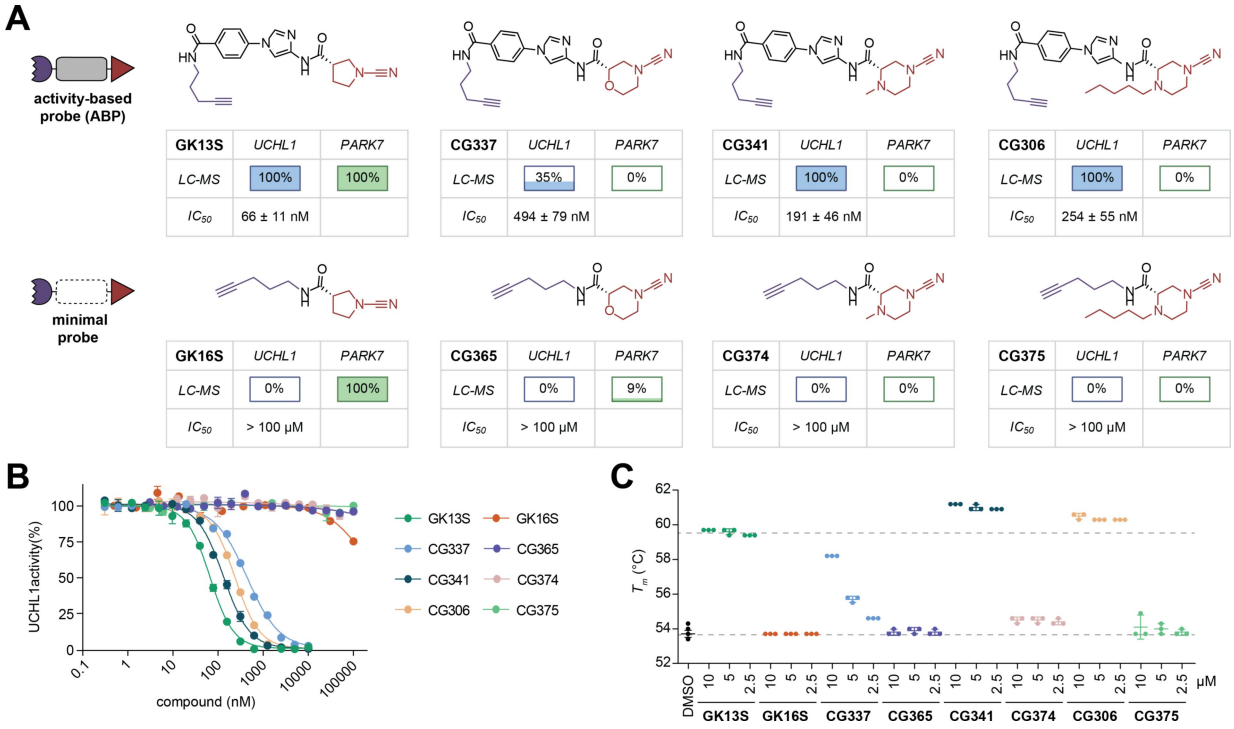

Figure 3. *N*-Cyanopiperazines show UCHL1 over PARK7 selectivity in vitro and retain UCHL1 potency. A.) Schematic representation of chemical structures comprising warhead (red), specificity element (grey) and alkyne handle (purple). Covalent protein modification as assessed by intact protein mass spectrometry is displayed as described in Figure 1, assayed by treating 3 µM UCHL1 or PARK7 with 10 µM compound or DMSO for 1 h. IC_{50} values of UCHL1 inhibition were derived from data shown in B. B.) Inhibitory potencies of indicated compounds, preincubated with UCHL1 for 1 h, as determined from a Ubiquitin-RhoG cleavage assay. Data points are shown as mean ± standard deviation (N = 3). C.) Thermal shift assay showing the protein melting temperature (T_m) of UCHL1 pre-treated for 1 h with compounds at indicated concentrations. Melting temperatures of apo and GK13S-bound UCHL1 are shown as grey lines.

achieve complete modification of compound-bound protein with the trifunctional linker, as observed through an upshift in the western blot for UCHL1 (Figure S7). To reduce the loss of cyanopiperazine-target conjugates due to the covalent-reversible nature of their linkage, the assay relied on shortened times for the bead incubation and washes. Probing the elution fractions for UCHL1 and PARK7, we observed that both cyanopiperazines CG341 and CG306 engaged only UCHL1, but not PARK7, which is fully consistent with the in vitro data (Figure 4D). As controls, we observed that GK13S engaged UCHL1 and PARK7, whereas GK16S engaged only PARK7. In line with the reversibility, the assay did not allow for preparative enrichment of UCHL1. Of note, while CG341 and CG306 possess very similar potencies on UCHL1 in vitro, CG306 seems to be of slightly higher potency in all cellular experiments (Figure 4A,4C,4D) which could be due to its more hydrophobic nature and a higher cell permeability. Taken together, these experiments demonstrated that cyanopiperazines potently and selectively inhibit UCHL1 in cells but unlike cyanopyrrolidines do not engage PARK7 and are therefore suitable to interrogate UCHL1-mediated cellular processes separately from PARK7.

Structural basis for recognition of N-cyanopiperazines by UCHL1

While the selectivity against PARK7 could be attributed to the change from a 5-membered to a 6-membered ring (see data on cyanopiperidine CG305), the gain in UCHL1 potency stemmed from the introduction of the alkylated nitrogen into the ring. To reveal the molecular basis for this improved potency (Figure 1G, Figure 3B) and protein interaction (Figure 3C) of the cyanopiperazines, we solved a crystal structure of human UCHL1 in covalent complex with CG341 to 2.20 Å resolution (Figure 5A, Figure S8A, Table S1). Utilizing lysine-methylated protein as previously for the structure with cyanopyrrolidine GK13S, crystallization proceeded with 10 copies in the asymmetric unit yet in a different crystal form (Table S1). All 10 copies were completely superimposable (Figure S8B) with a consistent binding mode of the compound (Figure S8C) and with very good electron density for entire inhibitor in all copies except for parts of the conformationally flexible alkyne tag (Figure S8D). The structure shows the isothiourea linkage of the cyanamide to the catalytic Cys90, which is stabilized by a hydrogen bond-donating amide of the Gln84 side chain and by a hydrogen bond accepting carbonyl backbone of Gly87 (Figure 5B). Additional polar contacts are made between peptide backbone amides and central parts of the inhibitor,

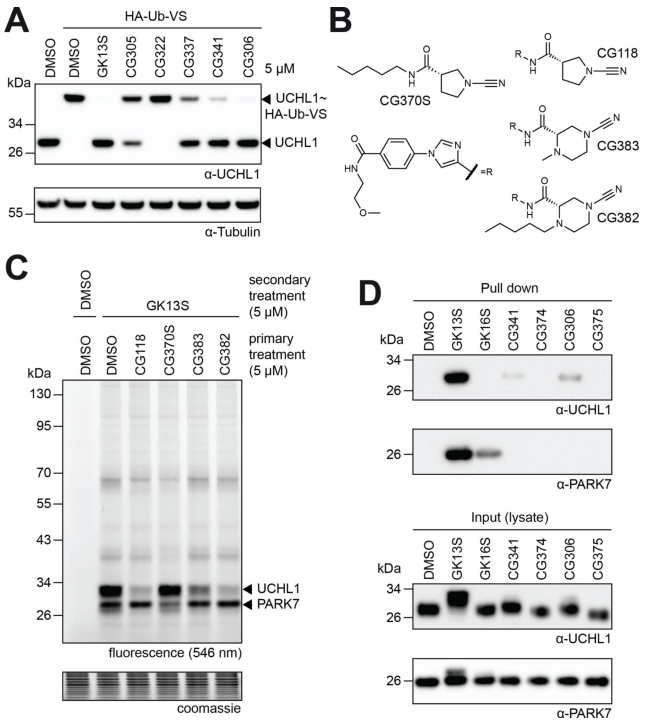

Figure 4. Cellular characterisation of piperidine-, morpholine- and piperazine-warhead analogues of GK13S. A.) Inhibition of cellular UCHL1. HEK293 cells were incubated with indicated compounds or DMSO for 24 h. Lysates were then treated with HA-Ub-VS probe where shown and analysed by western blot to assess UCHL1 engagement by compounds. B.) Structure of non-alkyne tagged probes. C.) Competition assay. HEK293 cells were treated with alkyne-free derivatives of GK13S (CG118), GK16S (CG370S), CG341 (CG383) and CG306 (CG382) for 24 h, to occupy their respective targets. A secondary treatment with GK13S for 24 h and subsequent fluorescence labelling visualized all targets still bound by GK13S. D.) Gel-based pull-down assay with GK13S, the piperazine warhead analogues and their corresponding minimal probes from HEK293 proteomes. Use of GK13S enriches UCHL1 together with the major off target PARK7, whereas the cyanopiperazine probes CG341 and CG306 weakly pull down UCHL1, but do not enrich PARK7. Uncropped versions of all blots are included in the SI.

e.g., between the tertiary amine and Phe160, between the amide and Phe160 and Met6, and of the imidazole nitrogen and Glu7 (Figure 5C). The phenyl ring of CG341 is contacted by a hydrophobic groove lined by Leu52 and Phe160, which is normally used for Leu73 recognition of Ubiquitin (Figure 5D, Figure S8E).

Superposition with a structure of UCHL1 bound to Ubiquitin revealed CG341 to occupy the substrate binding cleft of the enzyme in a manner similar to GK13S and with an identical compound-induced hybrid conformation. However, an important difference was observed regarding the cross-over loop, which spatially restricts access to the enzyme's active site:[38,39] While in the apo and GK13S-bound states the cross-over loop was disordered, clear electron density for the entire loop was observable in some copies in the CG341-bound structure. In all other copies, parts on either end of the loop were ordered. Moreover, the loop was found to adopt a conformation not previously observed. This compound-induced conformational restriction can be illustrated with Cys152, whose position changes by 10 Å compared to the Ubiquitin-bound state (Figure 5D) and which thus becomes part of the compound binding site. Superposition of UCHL1 structures in complex with GK13S and CG341 revealed how the additional atoms of the piperazine ring are accommodated (Figure 5E). The *N*-methyl group is contacted by a shallow hydrophobic pocket made of Pro5 and the now ordered Cys152 side chain (Figure 5F–G). The crossover loop located in 5 Å distance above the pocket explains how also the larger alkyl chain of CG306 is tolerated.

The structure illustrates why *N*-alkylated piperazines, but not piperidines and *N*-acylated piperazines, are potent UCHL1 inhibitors. Moreover, the observed conformational restriction is consistent with the higher protein stabilization of piperazines compared to their pyrrolidine analogues (Figure 3C). The binding mode is distinct to the ligand engagement observed in PARK7 (Figure 1C), where both carbons of the ring directly adjacent to the cyanamide are contacted by protein residues. Collectively, our data suggest that cyanopiperidines and cyanopiperazines are prevented from reaching the PARK7 catalytic cysteine due to the comparatively narrow active site environment. Moreover, they explain how the more open active site of UCHL1 favours cyanopyrrolidines but can accommodate the larger cyanopiperazines with a unique cross-over loop conformation and in full agreement with the experimental data.

DUB-wide specificity for UCHL1

Cyanopyrrolidine-based inhibitors were reported for USP30, UCHL1, JOSD1, USP7, and USP28—albeit often with cross-reactivity at higher concentration—, suggesting that this chemical warhead is a privileged structure for the covalent targeting of deubiquitinases.[7–14,24,25] In line with this observation, a pan-DUB-selective probe with a cyanopyrrolidine warhead was recently introduced,[7] raising the question how selectivity for individual DUBs of cyanamide-based compounds can be achieved. We therefore tested if cyanopiperazines not only decrease non-DUB targets, such as PARK7, of the respective cyanopyrrolidines, but also improve in-class selectivity among other DUBs.

We thus profiled both GK13S and CG341 in a commercial panel of 55 recombinant DUBs covering six enzyme classes present in humans (Figure 6A, Figure S9A–B).[40] We opted for high concentrations (approx. 75x times the in vitro IC_{50} values, i.e., 5 μM for GK13S and 15 μM for CG341S) in order to identify all likely off-target activity. Under those conditions, the cyanopyrrolidine GK13S inhibited six DUBs to more than 50 %, which in addition to UCHL1 included USP30, for which other cyanopyrrolidines have been identified as inhibitors, as well as the two USP9 variants, USP45 and JOSD2, for which selective nitrile-based inhibitors have not been reported yet. In contrast, the cyanopiperazine only inhibited UCHL1 to a similar degree. Considering the high concentration of the compound, the large size of the panel of DUBs and the high propensity of

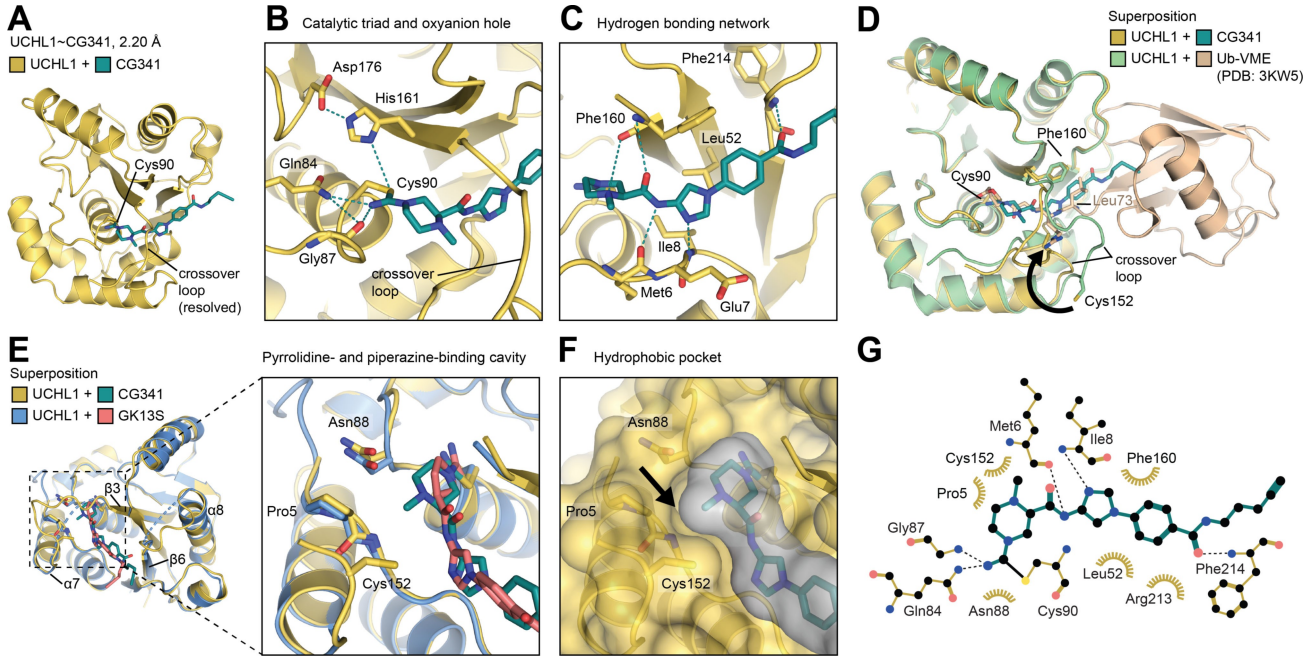

Figure 5. Crystal structure of UCHL1 in covalent complex with CG341. A.) Overview of the UCHL1~CG341 structure. The catalytic cysteine and the crossover loop are indicated. B.) Zoom into the binding site showing the catalytic triad (Cys90, His161, Asp176) and the oxy-anion hole (Gln84, Gly87) stabilizing the isothiourea linkage. Hydrogen bonds are shown with dashed lines. C.) Zoom into the hydrogen bonding network anchoring CG341 into the substrate binding cleft of UCHL1. D.) Superposition of UCHL1~CG341 structure with UCHL1 in complex with a Ubiquitin probe (Ub-VME). The change in conformation of the crossover loop including Cys152 is highlighted with a black arrow. E.) Superposition of cyanopyrrolidine (GK13S) and cyanopiperazine (CG341)-bound UCHL1, including zoom into the surrounding of the introduced tertiary amine. F.) View as in E but with surface representation to demonstrate the shallow hydrophobic pocket (black arrow) created by Pro5 and Cys152 and occupied by the *N*-methyl group of CG341. G.) Ligplot representation of CG341 interacting with UCHL1.

many of these to react with electrophilic fragments, this specificity is striking also in the context of previously recorded profiles.[8,10,19,41]

USP30 was the only other DUB with an activity below 90 %, displaying 72 % remaining activity. We validated these results by assessing USP30's ability to covalently bind the cyanamides. Intact protein mass spectrometry revealed partial modification of the catalytic domain of USP30 by 10 μM of GK13S, while the investigated cyanopiperazines did not cause protein-compound adducts (Figure 6B, Figure S10A–B). Moreover, we examined the inhibitory potential of the compounds on USP30, USP9X and USP45 using Ubiquitin-RhoG cleavage assays. While GK13S indeed showed inhibitory potency on all these DUBs with IC_{50} values in the low μM range, both cyanopiperazines showed either no inhibition (catalytic domain of USP9X, full length USP45) or weak inhibition with an IC_{50} above 10 μM (engineered catalytic domain of USP30) (Figure 6C). We validated the assay with previously reported inhibitors for USP30[12] and USP9X[42] (Figure 6D, Scheme S16) as well as the wild-type soluble USP domain of USP30 (Figure S10C). Importantly, full-length USP9X did not show inhibition by GK13S (Figure S10D), indicating that inhibition of USP9X by GK13S in the panel may be an artefact of the used catalytic domain. While the precise inhibition/protein modification numbers are difficult to compare across the different assay formats, buffers and protein batches, the data are overall in excellent agreement that cyanopiperazines are specific for UCHL1.

Lastly, we tested if the cyanopiperazines engage endogenous USP30 as the only partially inhibited DUB of the panel. We hence incubated HEK293 cells with compounds for 24 h and visualized their UCHL1 and USP30 target engagement in the Ubiquitin probe competition assay (Figure 6E). Consistent with the previous experiments, GK13S and both piperazines potently inhibited cellular UCHL1, whereas the USP30 inhibitor CG085 partially inhibited UCHL1. Conversely, we found that both cyanopiperazines did not inhibit cellular USP30, in contrast to CG085 and GK13S. These data demonstrate that these cyanopiperazines are specific inhibitors for UCHL1 in vitro as well as in cells.

Conclusion

We report the introduction of cyanopiperazines as unexplored covalent enzyme inhibitors with a high preference for the deubiquitinating enzyme UCHL1. The transition from 5-membered pyrrolidines to 6-membered heterocycles markedly improved compound specificity by eliminating binding to the protein deglycase PARK7 and by dampening reactivity with other DUBs, both in cells and in vitro. The data are consistent with other cyclic electrophilic moieties, for which target selectivity is encoded by ring-size.[43,44] Moreover, the transition introduced an unexpected and

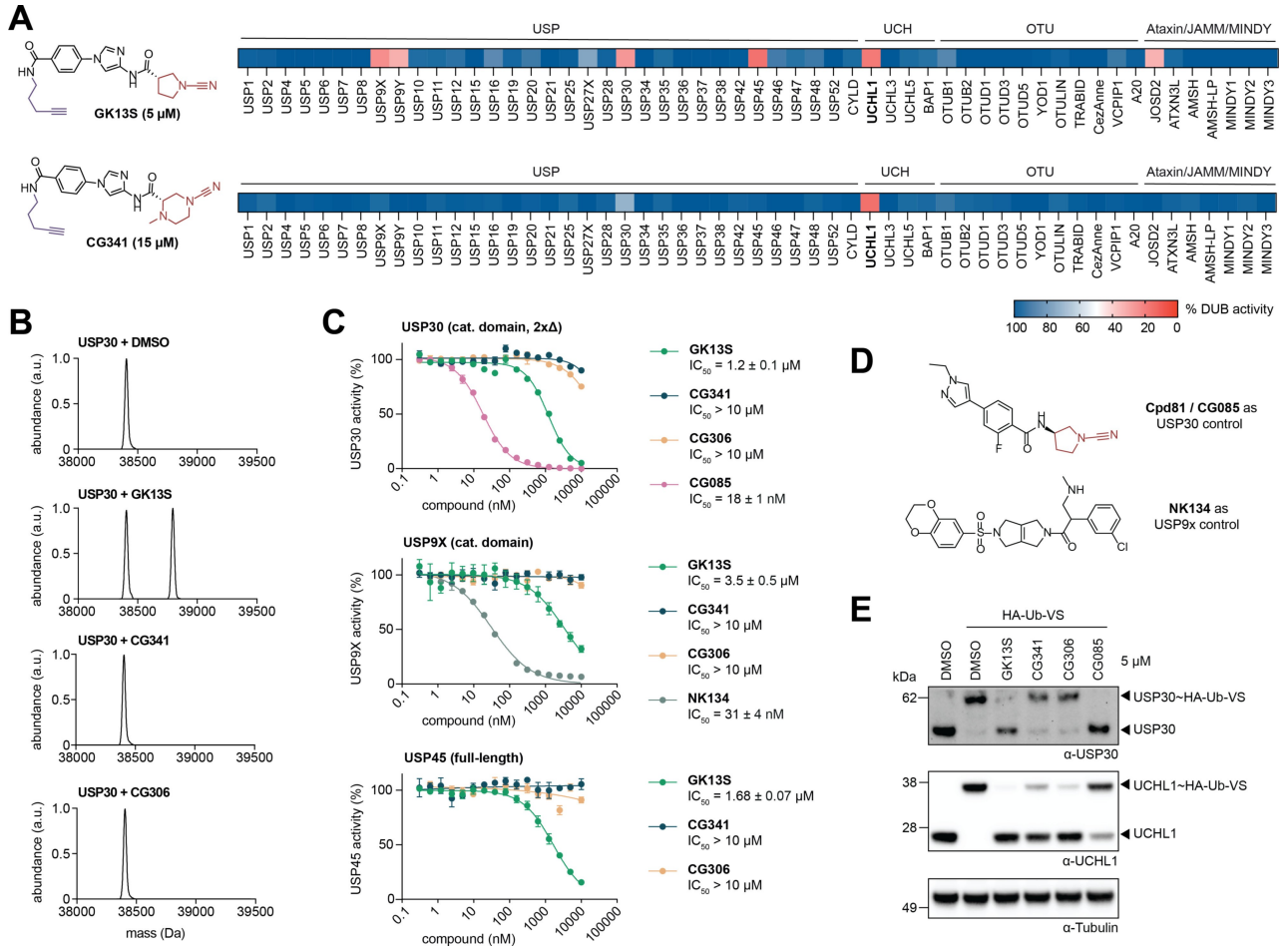

Figure 6. *N*-Cyanopiperazines display DUB-wide specificity for UCHL1 in vitro and in cells. A.) Results of DUB panel profiling. Recombinant human DUBs were preincubated with indicated compounds at given concentrations for 30 min. Remaining activities were determined by a MALDI-TOF-based substrate conversion assay and are shown as heatmaps. B.) Intact protein mass spectrometry of USP30 (cat. domain, 2xΔ construct) incubated with indicated compounds. C.) Ubiquitin-RhoG cleavage assays for USP30, USP9X and USP45, and indicated compounds. Data are given as mean ± standard deviation (N = 3). D.) Structures of USP30 and USP9X control inhibitors used in previous panel. E.) Cellular UCHL1 and USP30 inhibition assay. Intact HEK293 cells were treated with indicated compounds for 24 h. Lysates were incubated with HA-Ub-VS probe and endogenous UCHL1 and USP30 were visualized by western blot. Cyanopiperazines CG341 and CG306 show selective inhibition of UCHL1. Uncropped versions of all blots are included in the SI.

context-dependent reversibility of the isothiourea linkage of the compound to the catalytic cysteine of UCHL1, preventing efficient functionalisation of the probe through copper-catalysed click chemistry. Our data highlight an important caveat for the investigation of covalent small-molecule-protein isothiourea linkages. This property warrants further mechanistic investigations due to its implications for ongoing target discovery efforts of electrophilic nitriles. While the reversible nature of such linkages was demonstrated for a model cyanamide and papain protease,[21] quantitative analyses with the cyanopiperidine-based BTK inhibitor PF-303[1] and cyanopyrrolidine inhibitors of UCHL1[8,10,11] concluded that their binding mode is more akin to covalent-irreversible/covalent-slowly reversible with dissociation half-times of above 5 hours. Our data suggest that conditions established for cyanopyrrolidines cannot readily be transferred to cyanamides of cyanopiperazines. Bespoke workflows may be needed for unbiased, proteome-wide mass-spectrometry-based profiling studies with cyanopiperazines (e.g. lysate-based pulldowns of pre-functionalized, immobilized probes or the use of photo crosslinker-containing versions) and such assays are crucial for an assessment of selectivity against other cellular targets.[45] The characteristic of reversibility is loosely reminiscent of cysteine-targeted Michael Acceptors, for which rapidly reversible variants of high chemical similarity have been reported.[46]

Based on cellular target engagement, competitive labelling, and profiling of a panel of recombinant DUBs, we introduce the cyanopiperazines CG341 and CG306 for the selective perturbation of UCHL1 in cells. The reported crystal structure revealed a unique and compound-induced conformational restriction of the cross-over loop in UCHL1, which underlies the improved compound specify. Through biochemical and structural characterisation of the specificities of cyanamides of different ring sizes and substitutions, our data provide a framework for the rationalisation of the

protein target spectrum of bioactive compounds of this important class. Considering the high interest to identify and characterise novel electrophilic fragments with bioactivity in the ubiquitin system,[4,5,25,47,48] our work represents an encouraging case study for the refining of covalently acting compounds into specific chemical probes, bringing closer the rational optimization of reactive compounds and emphasizing the potential to engineer specificity through subtle chemical modifications around the warhead.

Supporting Information

Supporting Information containing experimental procedures, compound characterisation data, a supplementary Table and supplementary Figures is provided as a separate file.

Acknowledgements

We are grateful for support with crystallization, data collection and biophysics by beamline scientists at the Swiss Light Source (SLS) and by Dr. R. Gasper. We thank all members of the Gersch lab for discussions, advice, and reagents, and K. Gallant for help with Figure making. We acknowledge excellent support by all staff at TU Dortmund University and the Max Planck Institute, in particular by J. Hane, E. Crosson, L. Templin, F. Pfeffermann, and Prof. Dr. W. Hiller. This work was funded by Deutsche Forschungsgemeinschaft (DFG, German Research Foundation, Project-ID GE 3110/1-1—Emmy Noether; and Project-ID 424228829—SFB1430) and by the State of North Rhine-Westphalia through the 'CANcer TARgeting Network' initiative (NW21-062C). Work in the Gersch lab is further supported by AstraZeneca, Merck KGaA, Pfizer Inc., and the Max Planck Society as part of the Chemical Genomics Centre III (CGCIII-352S). Open Access funding enabled and organized by Projekt DEAL.

Conflict of Interest

All authors declare that they have no conflicts of interest.

Data Availability Statement

Data supporting the findings of this study are available in the supplementary material of this article. Data related to the crystal structures have been deposited with the protein data bank (PDB) under accession codes 8PW1, 8PQ0, and 8PPW.

Keywords: Ubiquitin · covalent inhibitors · proteases · protein structures · heterocycles

[1] M. Gehringer, S. A. Laufer, *J. Med. Chem.* **2019**, *62*, 5673–5724.
[2] R. Lagoutte, R. Patouret, N. Winssinger, *Curr. Opin. Chem. Biol.* **2017**, *39*, 54–63.
[3] L. E. Sanman, M. Bogyo, *Annu. Rev. Biochem.* **2014**, *83*, 249–273.
[4] N. J. Henning, L. Boike, J. N. Spradlin, C. C. Ward, G. Liu, E. Zhang, B. P. Belcher, S. M. Brittain, M. J. Hesse, D. Dovala, L. M. McGregor, R. Valdez Misiolek, L. W. Plasschaert, D. J. Rowlands, F. Wang, A. O. Frank, D. Fuller, A. R. Estes, K. L. Randal, A. Panidapu, J. M. McKenna, J. A. Tallarico, M. Schirle, D. K. Nomura, *Nat. Chem. Biol.* **2022**, *18*, 412–421.
[5] S. Ramachandran, N. Makukhin, K. Haubrich, M. Nagala, B. Forrester, D. M. Lynch, R. Casement, A. Testa, E. Bruno, R. Gitto, A. Ciulli, *Nat. Commun.* **2023**, *14*, 6345.
[6] E. Mons, R. Q. Kim, M. P. C. Mulder, *Pharmaceuticals* **2023**, *16*, 547.
[7] D. Conole, F. Cao, C. W. Am Ende, L. Xue, S. Kantesaria, D. Kang, J. Jin, D. Owen, L. Lohr, M. Schenone, J. D. Majmudar, E. W. Tate, *Angew. Chem. Int. Ed. Engl.* **2023**, *62*, e202311190.
[8] N. Panyain, A. Godinat, T. Lanyon-Hogg, S. Lachiondo-Ortega, E. J. Will, C. Soudy, M. Mondal, K. Mason, S. Elkhalifa, L. M. Smith, J. A. Harrigan, E. W. Tate, *J. Am. Chem. Soc.* **2020**, *142*, 12020–12026.
[9] N. Panyain, A. Godinat, A. R. Thawani, S. Lachiondo-Ortega, K. Mason, S. Elkhalifa, L. M. Smith, J. A. Harrigan, E. W. Tate, *RSC Med. Chem.* **2021**, *12*, 1935–1943.
[10] R. Kooij, S. Liu, A. Sapmaz, B. T. Xin, G. M. C. Janssen, P. A. van Veelen, H. Ovaa, P. T. Dijke, P. P. Geurink, *J. Am. Chem. Soc.* **2020**, *142*, 16825–16841.
[11] C. Grethe, M. Schmidt, G. M. Kipka, R. O'Dea, K. Gallant, P. Janning, M. Gersch, *Nat. Commun.* **2022**, *13*, 5950.
[12] A. Jones, M. Kemp, M. Stockley, K. Gibson, G. Whitlock, *WO2016156816 A1* **2016**.
[13] M. Kemp, M. Stockley, A. Jones, *US20180194724 A1* **2018**.
[14] M. Kemp, *Prog. Med. Chem.* **2016**, *55*, 149–192.
[15] M. J. Clague, S. Urbe, D. Komander, *Nat. Rev. Mol. Cell Biol.* **2019**, *20*, 338–352.
[16] I. E. Wertz, X. Wang, *Cell Chem. Biol.* **2019**, *26*, 156–177.
[17] S. M. Lange, L. A. Armstrong, Y. Kulathu, *Mol. Cell* **2022**, *82*, 15–29.
[18] A. Pinto-Fernandez, S. Davis, A. B. Schofield, H. C. Scott, P. Zhang, E. Salah, S. Mathea, P. D. Charles, A. Damianou, G. Bond, R. Fischer, B. M. Kessler, *Front. Chem.* **2019**, *7*, 592.
[19] T. Z. Fang, Y. Sun, A. C. Pearce, S. Eleuteri, M. Kemp, C. A. Luckhurst, R. Williams, R. Mills, S. Almond, L. Burzynski, N. M. Markus, C. J. Lelliott, N. A. Karp, D. J. Adams, S. P. Jackson, J. F. Zhao, I. G. Ganley, P. W. Thompson, G. Balmus, D. K. Simon, *Nat. Commun.* **2023**, *14*, 7295.
[20] M. W. Martin, A. J. Buckmelter, *WO2019222468A1* **2019**.
[21] J. P. Falgueyret, R. M. Oballa, O. Okamoto, G. Wesolowski, Y. Aubin, R. M. Rydzewski, P. Prasit, D. Riendeau, S. B. Rodan, M. D. Percival, *J. Med. Chem.* **2001**, *44*, 94–104.
[22] Y. H. Wang, F. Zhang, H. J. Diao, R. B. Wu, *ACS Catal.* **2019**, *9*, 2292–2302.
[23] D. R. Owen, C. M. N. Allerton, A. S. Anderson, L. Aschenbrenner, M. Avery, S. Berritt, B. Boras, R. D. Cardin, A. Carlo, K. J. Coffman, A. Dantonio, L. Di, H. Eng, R. Ferre, K. S. Gajiwala, S. A. Gibson, S. E. Greasley, B. L. Hurst, E. P. Kadar, A. S. Kalgutkar, J. C. Lee, J. Lee, W. Liu, S. W. Mason, S. Noell, J. J. Novak, R. S. Obach, K. Ogilvie, N. C. Patel, M. Pettersson, D. K. Rai, M. R. Reese, M. F. Sammons, J. G. Sathish, R. S. P. Singh, C. M. Steppan, A. E. Stewart, J. B. Tuttle, L. Updyke, P. R. Verhoest, L. Wei, Q. Yang, Y. Zhu, *Science* **2021**, *374*, 1586–1593.

[24] J. Yang, E. L. Weisberg, X. Liu, R. S. Magin, W. C. Chan, B. Hu, N. J. Schauer, S. Zhang, I. Lamberto, L. Doherty, C. Meng, M. Sattler, L. Cabal-Hierro, E. Winer, R. Stone, J. A. Marto, J. D. Griffin, S. J. Buhrlage, *Leukemia* **2022**, *36*, 210–220.
[25] W. C. Chan, X. Liu, R. S. Magin, N. M. Girardi, S. B. Ficarro, W. Hu, M. I. Tarazona Guzman, C. A. Starnbach, A. Felix, G. Adelmant, A. C. Varca, B. Hu, A. S. Bratt, E. DaSilva, N. J. Schauer, I. Jaen Maisonet, E. K. Dolen, A. X. Ayala, J. A. Marto, S. J. Buhrlage, *Nat. Commun.* **2023**, *14*, 686.
[26] M. L. Stockley, M. I. Kemp, A. Madin, *WO2018065768* **2018**.
[27] A. Tjaden, A. Chaikuad, E. Kowarz, R. Marschalek, S. Knapp, M. Schroder, S. Müller, *Molecules* **2022**, *27*, 1439.
[28] P. Bishop, D. Rocca, J. M. Henley, *Biochem. J.* **2016**, *473*, 2453–2462.
[29] A. T. Reinicke, K. Laban, M. Sachs, V. Kraus, M. Walden, M. Damme, W. Sachs, J. Reichelt, M. Schweizer, P. C. Janiesch, K. E. Duncan, P. Saftig, M. M. Rinschen, F. Morellini, C. Meyer-Schwesinger, *Proc. Natl. Acad. Sci. USA* **2019**, *116*, 7963–7972.
[30] I. Maniv, M. Sarji, A. Bdarneh, A. Feldman, R. Ankawa, E. Koren, I. Magid-Gold, N. Reis, D. Soteriou, S. Salomon-Zimri, T. Lavy, E. Kesselman, N. Koifman, T. Kurz, O. Kleifeld, D. Michaelson, F. W. van Leeuwen, B. M. Verheijen, Y. Fuchs, M. H. Glickman, *Nat. Commun.* **2023**, *14*, 5922.
[31] S. Liu, R. Gonzalez-Prieto, M. Zhang, P. P. Geurink, R. Kooij, P. V. Iyengar, M. van Dinther, E. Bos, X. Zhang, S. E. Le Devedec, B. van de Water, R. I. Koning, H. J. Zhu, W. E. Mesker, A. C. O. Vertegaal, H. Ovaa, L. Zhang, J. W. M. Martens, P. Ten Dijke, *Clin. Cancer Res.* **2020**, *26*, 1460–1473.
[32] Z. Liang, A. Damianou, I. Vendrell, E. Jenkins, F. H. Lassen, S. J. Washer, G. Liu, G. Yi, H. Lou, F. Cao, X. Zheng, R. A. Fernandes, T. Dong, E. W. Tate, E. D. Daniel, B. M. Kessler, *bioRxiv* **2023**, 2023.2010.2009.561576.
[33] G. Richarme, C. Liu, M. Mihoub, J. Abdallah, T. Leger, N. Joly, J. C. Liebart, U. V. Jurkunas, M. Nadal, P. Bouloc, J. Dairou, A. Lamouri, *Science* **2017**, *357*, 208–211.
[34] Y. Goto, L. Zeng, C. J. Yeom, Y. Zhu, A. Morinibu, K. Shinomiya, M. Kobayashi, K. Hirota, S. Itasaka, M. Yoshimura, K. Tanimoto, M. Torii, T. Sowa, T. Menju, M. Sonobe, H. Kakeya, M. Toi, H. Date, E. M. Hammond, M. Hiraoka, H. Harada, *Nat. Commun.* **2015**, *6*, 6153.
[35] X. Tao, L. Tong, *J. Biol. Chem.* **2003**, *278*, 31372–31379.
[36] Y. Jia, R. Q. Kim, R. Kooij, H. Ovaa, A. Sapmaz, P. P. Geurink, *J. Med. Chem.* **2022**, *65*, 13288–13304.
[37] S. Tashiro, J. M. M. Caaveiro, M. Nakakido, A. Tanabe, S. Nagatoishi, Y. Tamura, N. Matsuda, D. Liu, Q. Q. Hoang, K. Tsumoto, *ACS Chem. Biol.* **2018**, *13*, 2783–2793.
[38] Z. R. Zhou, Y. H. Zhang, S. Liu, A. X. Song, H. Y. Hu, *Biochem. J.* **2012**, *441*, 143–149.
[39] D. A. Boudreaux, T. K. Maiti, C. W. Davies, C. Das, *Proc. Natl. Acad. Sci. USA* **2010**, *107*, 9117–9122.
[40] V. De Cesare, J. Moran, R. Traynor, A. Knebel, M. S. Ritorto, M. Trost, H. McLauchlan, C. J. Hastie, P. Davies, *Nat. Protoc.* **2020**, *15*, 4034–4057.
[41] E. V. Rusilowicz-Jones, J. Jardine, A. Kallinos, A. Pinto-Fernandez, F. Guenther, M. Giurrandino, F. G. Barone, K. McCarron, C. J. Burke, A. Murad, A. Martinez, E. Marcassa, M. Gersch, A. J. Buckmelter, K. J. Kayser-Bricker, F. Lamoliatte, A. Gajbhiye, S. Davis, H. C. Scott, E. Murphy, K. England, H. Mortiboys, D. Komander, M. Trost, B. M. Kessler, S. Ioannidis, M. K. Ahlijanian, S. Urbe, M. J. Clague, *Life Sci Alliance* **2020**, *3*, e202000768.
[42] M. Lynes, W. Wang, *WO2020191022 A1* **2020**.
[43] T. Böttcher, M. Pitscheider, S. A. Sieber, *Angew. Chem. Int. Ed. Engl.* **2010**, *49*, 2680–2698.
[44] A. Mahia, A. E. Kiib, M. Nisavic, E. B. Svenningsen, J. Palmfeldt, T. B. Poulsen, *Angew. Chem. Int. Ed. Engl.* **2023**, *62*, e202304142.
[45] K. Senkane, E. V. Vinogradova, R. M. Suciu, V. M. Crowley, B. W. Zaro, J. M. Bradshaw, K. A. Brameld, B. F. Cravatt, *Angew. Chem. Int. Ed.* **2019**, *58*, 11385–11389.
[46] I. M. Serafimova, M. A. Pufall, S. Krishnan, K. Duda, M. S. Cohen, R. L. Maglathlin, J. M. McFarland, R. M. Miller, M. Frodin, J. Taunton, *Nat. Chem. Biol.* **2012**, *8*, 471–476.
[47] R. Cookson, A. Vuorinen, J. Pettinger, C. R. Kennedy, J. M. Kirkpatrick, R. E. Peltier-Heap, A. Powell, A. P. Snijders, M. Skehel, D. House, K. Rittinger, J. T. Bush, *Cell Rep Phys Sci* **2023**, *4*, 101636.
[48] E. Resnick, A. Bradley, J. Gan, A. Douangamath, T. Krojer, R. Sethi, P. P. Geurink, A. Aimon, G. Amitai, D. Bellini, J. Bennett, M. Fairhead, O. Fedorov, R. Gabizon, J. Gan, J. Guo, A. Plotnikov, N. Reznik, G. F. Ruda, L. Diaz-Saez, V. M. Straub, T. Szommer, S. Velupillai, D. Zaidman, Y. Zhang, A. R. Coker, C. G. Dowson, H. M. Barr, C. Wang, K. V. M. Huber, P. E. Brennan, H. Ovaa, F. von Delft, N. London, *J. Am. Chem. Soc.* **2019**, *141*, 8951–8968.

Manuscript received: December 7, 2023
Accepted manuscript online: January 19, 2024
Version of record online: February 9, 2024